Available online at www.sciencedirect.com
ScienceDirect
Expert Systems with Applications 32 (2007) 1168–1182
Expert Systems with Applications
www.elsevier.com/locate/eswa

Decoupled control using neural network-based sliding-mode controller for nonlinear systems

Lon-Chen Hung, Hung-Yuan Chung *

Department of Electrical Engineering, National Central University, Jhong-Li, Tao-Yuan 320, Taiwan, ROC

Abstract

In this paper, an adaptive neural network sliding-mode controller design approach with decoupled method is proposed. The decoupled method provides a simple way to achieve asymptotic stability for a class of fourth-order nonlinear system. The adaptive neural sliding-mode control system is comprised of neural network (NN) and a compensation controller. The NN is the main regulator controller, which is used to approximate an ideal computational controller. The compensation controller is designed to compensate for the difference between the ideal computational controller and the neural controller. An adaptive methodology is derived to update weight parts of the NN. Using this approach, the response of system will converge faster than that of previous reports. The simulation results for the cart–pole systems and the ball–beam system are presented to demonstrate the effectiveness and robustness of the method. In addition, the experimental results for seesaw system are given to assure the robustness and stability of system.

Keywords: Neural; Sliding-mode control

1. Introduction

Various implementation methodologies for sliding-mode controllers exist today. The variable structure control (VSC) with sliding-mode, or sliding-mode control (SMC), is one of the effective nonlinear robust control approaches since it provides the system dynamics with an invariance property to uncertainties once the system dynamics are controlled in the sliding-mode (Utkin, 1977; Weibing, Wang, & Homaifa, 1995). It possesses many advantages including: (i) insensitivity to parameter variations; (ii) external disturbance rejection; and (iii) fast dynamic responses. However, there is undesirable chattering in the control effort and bounds on the uncertainties are required in the design of the SMC. The uncertainties usually include unmodel dynamics, parameter variations and external disturbances, etc. If the actual bounds of the uncertainties exceed the assumed values designed in the controller, the stability of the system in not guaranteed. Like other conventional control structures, the design of sliding-mode controllers needs the knowledge of the mathematical model of the plant, which decreases the performance in some applications where the mathematical modeling of the system is very hard and where the system has a large range of parameter variation together with unexpected and sudden external disturbances. That controller should also adapt itself to large parameter variations and to unexpected external disturbances (Bartolini, Punta, & Zolezzi, 2004; Buckner, 2002). For those cases we need a controller are generally called "intelligent" controllers. These controllers mainly work on the principals of fuzzy-logic, neural network (NN), genetic algorithms, etc. The idea of combining these intelligent control structures with sliding-mode approach attracted many researches (Barambones & Etxebarria, 2002; Horng, 1999; Hussain & Ho, 2004; Lin & Hsu, 2002; Lo & Kuo, 1998; Parma, de Menezes, & Braga, 1998; Wai, 2003; Xu, Sun, & Sun, 1996).

* Corresponding author. Tel.: +886 3 4227151x34475; fax: +886 3 4225830.
E-mail address: hychung@ee.ncu.edu.tw (H.-Y. Chung).

0957-4174/$ - see front matter © 2006 Published by Elsevier Ltd.
doi:10.1016/j.eswa.2006.02.024

Recently, NN-based stable and on-line adaptive control has been paid much attention in NN applications in robot control of trajectory tracking (Barambones & Etxebarria, 2002; Wai, 2003; Xu et al., 1996). These researches have two common features: (1) locally generalizing network are usually used for fast learning or adaptation, examples of this class of network include the Gaussian radial basis function (RBF) like nets (Lin & Chen, 1994) neural network combined with sliding-mode control design and (Huang, Huang, & Chiou, 2003) are used to design the RBF neural network with adaptive control architecture for the active dynamic absorber system. The basis spline network and a certain class of fuzzy logic network (Huang, Tan, & Lee, 2000) applied to friction compensation. The cerebellar model articulation controller (CMAC) (Abdelhameed, Pinspon, & Cetinkunt, 2002) used to the piezoelectric actuated tool post. (2) Lyapunov stability theory or passive theory is employed to design a closed loop control system, thus providing global stability (Hussain & Ho, 2004).

In this paper, we develop a decoupled sliding-mode control (DSMC) design strategy based on NN. The weights of the NN are changed according to some adaptive algorithm for the purpose of controlling the system states to hit an user-defined sliding surface and then slide along it. The initial weights of the NN can be set to small random numbers, and then on-line tuned, no supervised learning procedures are needed. This makes NN suitable for the nonlinear dynamic system control.

A decoupled neural network-based sliding-mode control (DNNSMC) design scheme is presented. An adaptive law is employed to on-line adjust the weights by using the reaching condition of a specified sliding surface. Since the proposed structure is able to learn the weights of the NN continuously, the initial weights can be started from zero for a class of fourth-order nonlinear systems. Each subsystem, which is decoupled into two second-order systems, is said to have main and sub-control purpose. Two sliding surfaces are constructed through the state variables of the decoupled subsystem. We define main and sub-target condition for these sliding surfaces, and introduce an intermediate variable from the sub-sliding surface condition. The proposed adaptation law, which results from the direct adaptive approach, is used to appropriately determine the weight of the unknown system variables.

The on-line adjust algorithm is derived in the Lyapunov sense; thus, the stability of the control system can be guaranteed. Furthermore, to relax the requirement for the uncertain bound in the compensation controller, an estimation mechanism is investigated to observe the uncertain bound, so that the chattering phenomena of the control efforts can be relaxed.

We proposed the DNNSMC has the following advantages: (1) It can control most of complex systems well without knowing their exact mathematical models. (2) The dynamic behavior of the controlled system can be approximately dominated by an hybrid sliding surface. (3) The DNNSMC can increase the robustness to system uncertainties better than conventional sliding-mode controller. (4) Our control approach has the advantage over the model-based control scheme to the former that it does require a prior knowledge of dynamic nonlinear system.

The rest of the paper is divided into five sections. In Section 2, the systems are described and problem formulation. In Section 3, design decoupled neural network sliding-mode controller is described. In Section 4, the proposed controller is used to control a single-inverted pendulum system, a double-inverted pendulum system and a ball–beam system and to show how the controller is synthesized as a C++ code with integrated into the software executed by the computer that controls the seesaw system. Finally, we conclude with Section 5.

2. System description

Consider a second-order nonlinear system, which can be represented by the following state-space model in a canonical form:

$$\begin{aligned}\dot{x}_1(t) &= x_2(t)\\ \dot{x}_2(t) &= f(\mathbf{x}) + b(\mathbf{x})u + d(t)\\ y(t) &= x_1(t)\end{aligned} \tag{1}$$

where $\mathbf{x} = [x_1 \;\; x_2]^{\mathrm{T}}$ is the state vector, $f(\mathbf{x})$ and $b(\mathbf{x})$ are nonlinear functions, u is the control input, and $d(t)$ is the external disturbance. The disturbance is assumed to be bounded as $|d(t)| \leqslant D(t)$.

For this kind of the second order system, we can use many kinds of control methods, such as, fuzzy control, PID control, sliding-mode control, etc. A control law u can be easily designed to make the second order system (1) arrive at our control goal. However, for such nonlinear models as a cart–pole system, the system dynamic representation is generally not in a canonical form exactly. Rather, it has a form shown below:

$$\begin{aligned}\dot{x}_1(t) &= x_2(t)\\ \dot{x}_2(t) &= f_1(\mathbf{x}) + b_1(\mathbf{x})u_1 + d_1(t)\\ \dot{x}_3(t) &= x_4(t)\\ \dot{x}_4(t) &= f_2(\mathbf{x}) + b_2(\mathbf{x})u_2 + d_2(t)\end{aligned} \tag{2}$$

where $\mathbf{x} = [x_1 \;\; x_2 \;\; x_3 \;\; x_4]^{\mathrm{T}}$ is the state vector, $f_1(\mathbf{x}), f_2(\mathbf{x})$ and $b_1(\mathbf{x})$, $b_2(\mathbf{x})$ are nonlinear functions, u_1, u_2 are the control inputs, and $d_1(t)$, $d_2(t)$ are external disturbances. The disturbances are assumed to be bounded as $|d_1(t)| \leqslant D_1(t)$, $|d_2(t)| \leqslant D_2(t)$. From (2), one can design u_1 and u_2 respectively, however, this approach is only utilized to control a subsystem in (2). For example, if the model is a cart–pole system, we only control either the pole or the cart of a system such as (2). Hence, the idea of decoupled is employed to design a control u to govern the whole system.

In Eq. (2), we first define one switching line as

$$s_1 = c_1(x_1 - z) + x_2 = [c_1 1][x_1 \quad x_2]^{\mathrm{T}} - c_1 z = \mathbf{c}^{\mathrm{T}}\mathbf{x}_{12} - c_1 z \tag{3}$$

and another switching line as

$$s_2 = c_2 x_3 + x_4 \tag{4}$$

In the design of decoupled sliding-mode controller, an equivalent control is first given so that the states can stay on sliding surface. Thus, in sliding motion, the system dynamic is independent of the original system and a stable equivalent control system is achieved. The equivalent control can be obtained by letting $\dot{s}_1$ equal to zero. That is

$$\dot{s}_1 = c_1(\dot{x}_1 - \dot{z}) + \dot{x}_2 = c_1 x_2 - c_1 \dot{z} + f_1 + b_1 u + d_1 = 0 \tag{5}$$

The decoupled sliding-mode control input is to be chosen as follows for a Lyapunov function candidate

$$V = \frac{1}{2} s_1 s_1^2 \tag{6}$$

Take the time derivative of (6) we have

$$\dot{V} = s_1 \dot{s}_1 = s_1(c_1 x_2 - c_1 \dot{z} + f_1 + b_1 u + d_1) \tag{7}$$

It can be easily shown from (7) that the decoupled sliding-mode controller u can be divided into an equivalent control input and a reaching mode control input if has the following form, will be negative:

$$u = u_{\text{eq}} - M \cdot \text{sgn}(s_1/\Phi_1), \quad \text{where } M > D_1(t)/|b_1(t)| \tag{8}$$

where M is a positive constant, then the system is controlled in such a way that the state always moves toward the sliding surface and hit it. Thus, the trajectory is always forced to move toward the sliding surface. But, (8) will have high-frequency switching near the sliding surface ($s_1 = 0$) due to the 'sgn' function involved. Thus, in order to reduce the chattering phenomena, we replace $\text{sgn}(s_1)$ with $\text{sat}(s_1)$ as follows:

$$u = u_{\text{eq}} - M \cdot \text{sat}(s_1) \tag{9}$$

Hence, in the sliding motion, an equivalent controller will be

$$u_{\text{eq}} = \frac{1}{b_1}(-c_1 x_2 + c_1 \dot{z} - f_1 + \dot{s}_1 + k s_1) \tag{10}$$

Substituting Eq. (10) into Eq. (5), we obtain

$$\dot{s}_1 + k s_1 = 0 \tag{11}$$

where k is a positive value, the sliding surface on the phase plane can be defined as (3). The control objective is to drive the system state to the original equilibrium point. The switching line variables s_1 and s_2 are reduced to zeros gradually at the same time by an intermediate variable z. In Eq. (3), z is a value transferred from s_2, it has a value proportional to s_2 and has the range proper to x_1. Eq. (3) denotes that the control objective of u_1 is changed from $x_1 = 0$, $x_2 = 0$ to $x_1 = z$, $x_2 = 0$ (Lo & Kuo, 1998).

Because the controller $u = u_1$ is used to govern the whole system, the bound of x_1 can be guaranteed by letting

$$|z| \leqslant Z_{\text{upper}}, \quad 0 < Z_{\text{upper}} < 1 \tag{12}$$

where Z_{upper} is the upper bound of abs(z). Eq. (12) implies that the maximum absolute value of x_1 will be limited.

Summarizing what we have mentioned above, z can be defined as

$$z = \text{sat}(s_2/\Phi_z) \cdot Z_{\text{upper}}, \quad 0 < Z_{\text{upper}} < 1 \tag{13}$$

where Φ_z is the boundary layer of s_2 to smooth z, Φ_z transfers s_2 to the proper range of x_1, and the definition of sat($\cdot$) function is

$$\text{sat}(\varphi) = \begin{cases} \text{sgn}(\varphi) & \text{if } |\varphi| \geqslant 1 \\ \varphi & \text{if } |\varphi| < 1 \end{cases} \tag{14}$$

Notice that z is a decaying oscillation signal because Z_{upper} is a factor less than one.

Remark 1. Consider Eq. (3). If $s_1 = 0$, then $x_1 = z$, $x_2 = 0$. Since z is a value transferred from s_2, when $s_2 \to 0$, then $z \to 0$ and $x_1 \to 0$. From Eq. (4), if the condition $s_1 \to 0$, the control objective can be achieved. Moreover, the choice of c_1 and c_2 has strong influence on the behavior in the transient state of the system. Appropriate choice of sliding factor is necessary for achieving favorable transient response.

If the perfect control law cannot obtain, it is not possible to implement (9). To overcome such a problem, a novel approach of the weight adaptation of the NN control is proposed to estimate an equivalent control input u_{eq}. This will be proposed in Section 3.

3. Design of decoupled neural network sliding-mode controller

In this section, we show how to develop a decoupled neural network sliding-mode controller for obtaining the equivalent control through weight adaptation. Then, we construct the hitting control to guarantee the stability of system. If the state trajectory can be forced to slide on sliding surface, then a stable equivalent control system is achieved. However, if the function f_1 is unknown (for simplicity, we assume b_1 is known), there is no way to yield equivalent control u_{eq}. In this paper, a set of neural network base is applied to approximating (9). Motivated by the principle of DSMC, the control law consists of the following two parts; one is the estimated sliding component u_{DNNSMC} that constructed by an adaptive mechanism. The effect of this term is to force the system state to slide on the sliding surface. Another is the hitting control u_h that drives the states toward the sliding surface.

3.1. Basic idea of NN approximation

Here, we employ a simple two-layer NN to approximate a general smooth nonlinear function on a compact set $S \in R^P$. According to the NN approximation property (Derks, Pastor, & Buydens, 1995; Liu, Zuo, & Meng, 2003), we have

$$f(\mathbf{x}) = \mathbf{w}^{\text{T}} \sigma(\mathbf{v}^{\text{T}} \mathbf{x}) + \varepsilon(\mathbf{x}) \tag{15}$$

where $\mathbf{x} = [1 \ x_1 \ \cdots \ x_p]^{\text{T}}$ is the input to NN, $\sigma(\cdot)$ is an active function, where $\mathbf{w} = [w_1 \ w_2 \ \cdots \ w_m]^{\text{T}}$ and $\mathbf{v} =$

$[v_1\ v_2\ \cdots\ v_m]^{\mathrm{T}}$ defined as the collection of NN weights for the output and the hidden layer, respectively, and $\varepsilon(\mathbf{x})$ is the NN approximation error. Define the NN weights error $\tilde{\mathbf{w}} = \hat{\mathbf{w}} - \mathbf{w}^*$, $\tilde{\mathbf{v}} = \hat{\mathbf{v}} - \mathbf{v}^*$ ("$\hat{}$" represents estimation value), denote the norm of a vector $\mathbf{x}$ is defined by $\|\mathbf{x}\| = \sqrt{\mathbf{x}^{\mathrm{T}}\mathbf{x}}$.

Assuming that $f(\mathbf{x})$ is continuous function and absolutely integrable, in the sense that

$$\int_{-\infty}^{\infty} |f(\mathbf{x})| \mathrm{d}x \leqslant c \quad \text{for } x \in R^{p+1} \tag{16}$$

where c is a sufficiently large positive constant. We can establish the following approximation theorem by Lemma 1.

Lemma 1. *For every function $f(\mathbf{x})$ satisfying (16) and every sigmoidal function $\sigma(\mathbf{x}) = 1/(1 + \exp(-\mathbf{x}))$, if $\xi \geqslant n$ (n is the number of the hidden-layer neurons), there exists an NN functional estimate $f_n(\mathbf{x}) = \mathbf{w}^{\mathrm{T}}\sigma(\mathbf{v}^{\mathrm{T}}\mathbf{x}) \in M_{\sigma,\xi}$ such that*

$$\|\varepsilon(\mathbf{x})\| \leqslant \mathrm{O}^2(n) + \|f(0)\| \tag{17}$$

where $M_{\sigma,\xi} = \{\mu\sigma(\xi(ax + b))\}$.

Proof. Consider (15) and let

$$\bar{f}(\mathbf{x}) = f(\mathbf{x}) - f(0) \tag{18}$$

the proof of Lemma 1 can be completed based on Theorem 1 in Barron (1993). □

Remark 2. Lemma 1 indicates that, for a special two-layer NN, the upper bound of NN functional reconstruction error is affected by NN structure (i.e. the number of hidden-layer neurons) and also related to the initial value of the estimated function.

3.2. Neural network base decoupled sliding-mode control

A single-hidden-layer NN with two layers of adjustable weights is indication in Fig. 1. Following the notation used in (Hornik, Stinchombe, & White, 1989; Lin & Hsu, 2002) the output of this NN takes the form

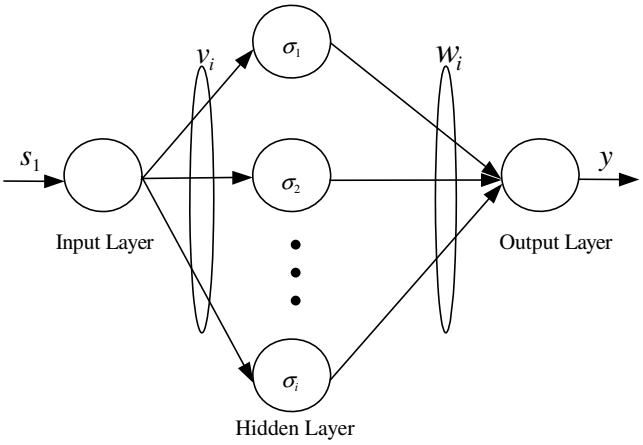

Fig. 1. A single-hidden-layer NN with two layers.

$$y = \sum_{i=1}^{m} w_i \sigma(v_i s_1) \tag{19}$$

where v_i and w_i are the input and y is output of the NN, respectively; $\sigma(\cdot)$ represents the hidden-layer activation function; v_i are the interconnection weights between the input and the hidden layers; and w_i are the interconnection weights between the hidden and the output layers. This architecture has one input, hidden-layer neurons, and one output. The activation function is considered as a sigmoid function

$$\sigma(s_1) = \frac{1}{(1 + \mathrm{e}^{-s_1})} \tag{20}$$

By collecting all the weights of the NN, (20) can be expressed in a vector form as

$$y = \mathbf{w}^{\mathrm{T}}\sigma(\mathbf{v}s_1) \tag{21}$$

A main property of a NN regarding feedback control purpose is the universal function approximation property. A NN is capable of approximating any smooth function to any desired accuracy, provided the number of hidden-layer neurons is sufficiently large.

By the universal approximation theorem (Chen & Chen, 1995), there exists ideal weight vectors $\mathbf{w}^*$ and $\mathbf{v}^*$ such that

$$\Omega = y^*(s_1, \mathbf{w}^*, \mathbf{v}^*) + \Delta = \mathbf{w}^{*T}\sigma(\mathbf{v}^* s_1) + \Delta \tag{22}$$

where Δ is the approximation error, which generally decreases as the net size increases. For any choice of a positive number Δ_k, one can find a feedforward NN such that $|\Delta| \leqslant \Delta_k$ for all s_1. The ideal NN weights in vectors and that are needed to best approximate a given nonlinear function are difficult to determine. In fact, they may not even be unique. However, all one needs to know for control purposes is that for a specified value of Δ_k, some ideal approximating NN weights exists. Then, an estimate of Ω can be given by

$$\hat{\Omega} = \hat{y}(s_1, \hat{\mathbf{w}}, \hat{\mathbf{v}}) = \hat{\mathbf{w}}^{\mathrm{T}}\sigma(\hat{\mathbf{v}}s_1) \tag{23}$$

where $\hat{\mathbf{w}}$ and $\hat{\mathbf{v}}$ are the estimated values of the ideal NN weights $\mathbf{w}^*$ and $\mathbf{v}^*$ that are provided by online weights tuning algorithms subsequently to be detailed. The $\sigma(\mathbf{v}^* s_1) = [\sigma_1^*\ \sigma_2^*\ \cdots\ \sigma_m^*]^{\mathrm{T}}$ are denoted with

$$\sigma_i^* = \frac{1}{(1 + \mathrm{e}^{-\mathbf{v}^* s_1})} = \frac{1}{(1 + \mathrm{e}^{-\hat{\mathbf{v}} s_1})} \tag{24}$$

The estimation errors of the weights of NN are defined as

$$\tilde{\mathbf{w}} = \hat{\mathbf{w}} - \mathbf{w}^*, \quad \tilde{\mathbf{v}} = \hat{\mathbf{v}} - \mathbf{v}^* \tag{25}$$

and the hidden-layer output error is given as

$$\tilde{\sigma} = \sigma(\mathbf{v}^* s_1) - \sigma(\hat{\mathbf{v}} s_1) \tag{26}$$

From the function $\sigma(\cdot)$ with parameter $\mathbf{x}^*$, one may write its Taylor series with another parameter

$$\sigma(\mathbf{x}^*) = \sigma(\hat{\mathbf{x}}) + \sigma'(\hat{\mathbf{x}})\tilde{\mathbf{x}} + \mathrm{O}^2(\tilde{\mathbf{x}}) \tag{27}$$

where σ' is the Jacobian, and the last term indicates terms of order $\tilde{\mathbf{x}}^2$. Therefore,

$$\tilde{\sigma} = \sigma'(\hat{\mathbf{v}}s_1)\tilde{\mathbf{v}}s_1 + \mathrm{O}^2(\tilde{\mathbf{v}}s_1) \tag{28}$$

The control law for the DNNSMC system, as shown in Fig. 2 is assumed to make the following form:

$$u(s_1, \hat{\mathbf{w}}, \hat{\mathbf{v}}) = u_{\mathrm{DNNSMC}} + u_h \tag{29}$$

where u_{DNNSMC} is the approximate equivalent control, and the hitting control u_h is designed to stabilized the states of the control system around a pre-selected uncertainty bound.

Substituting Eq. (29) into Eq. (2), we can obtain

$$\begin{aligned}\dot{x}_2 &= f_1(\mathbf{x}) + b_1(\mathbf{x})u \\ &= f_1(\mathbf{x}) + b_1(\mathbf{x})(u_{\mathrm{DNNSMC}} + u_h - u_{\mathrm{eq}}) \\ &= -c_1 x_2 + c_1\dot{z} + b_1(\mathbf{x})(u_{\mathrm{DNNSMC}} + u_h - u_{\mathrm{eq}})\end{aligned} \tag{30}$$

or, equivalently

$$\dot{\mathbf{x}}_{12} = \mathbf{A}_c\mathbf{x}_{12} + \mathbf{b}_c(u_{\mathrm{DNNSMC}} + u_h - u_{\mathrm{eq}}) + \mathbf{g}\dot{z} + \boldsymbol{\gamma}s_1 \tag{31}$$

where $\mathbf{x}_{12} = [x_1 \ x_2]^{\mathrm{T}}, \mathbf{A}_c = \begin{bmatrix} 0 & 1 \\ 0 & -c_1 \end{bmatrix}, \mathbf{b}_c = [0 \ b_1(\mathbf{x})]^{\mathrm{T}}, \mathbf{g} = [0 \ c_1]^{\mathrm{T}}, \boldsymbol{\gamma} = [0 \ -k]^{\mathrm{T}}$.

A boundary layer neighbouring the sliding surface is now defined as

$$s_{\Delta} = s_1 - \Phi_1 \cdot \mathrm{sat}(s_1/\Phi_1) \tag{32}$$

where Φ_1 is the boundary layer thickness. The system is now longer forced to stay in the decoupled sliding-mode but is constrained within the sliding layer $|s_1| \leqslant \Phi_1$. If $|s_1| < \Phi_1$, that is inside the boundary layer, $\dot{s}_{\Delta} = s_{\Delta} = 0$, while if $|s_1| > \Phi_1$, then $\dot{s}_{\Delta} = s_{\Delta}$ and $|s_{\Delta}| = |s_1| - \Phi_1$.

Hence, the (5) can be rewritten

$$\begin{aligned}\dot{s}_{\Delta} &= \mathbf{c}^{\mathrm{T}}\dot{\mathbf{x}}_{12} - c_1 z \\ &= \mathbf{c}^{\mathrm{T}}\mathbf{A}_c\mathbf{x}_{12} + \mathbf{c}^{\mathrm{T}}\mathbf{b}_c(u_{\mathrm{DNNSMC}} + u_h - u_{\mathrm{eq}}) + \mathbf{c}^{\mathrm{T}}\boldsymbol{\gamma}s_1 \\ &\quad + \mathbf{c}^{\mathrm{T}}\mathbf{g}z - c_1\dot{z} \\ &= b_1(u_{\mathrm{DNNSMC}} + u_h - u_{\mathrm{eq}}) - ks_{\Delta}\end{aligned} \tag{33}$$

where $\mathbf{c} = [c_1 \ 1]^{\mathrm{T}}$.

The above properties of the boundary layer concept are to be exploited, in the design of DNNSMC system, our goal being to chase adaptation as soon as the boundary layer is reached. This approach aims to avoid the possibility of unbounded growth.

Define the NN controller estimation error as $\tilde{\mathrm{u}}_{\mathrm{DNNSMC}}$ as

$$\begin{aligned}\tilde{u}_{\mathrm{DNNSMC}} &= u_{\mathrm{eq}} - u_{\mathrm{DNNSMC}} \\ &= u^*_{\mathrm{DNNSMC}} + \Delta - u_{\mathrm{DNNSMC}} \\ &= \mathbf{w}^{*T}\sigma(\mathbf{v}^*s_1) - \hat{\mathbf{w}}^{\mathrm{T}}\sigma(\hat{\mathbf{v}}^{\mathrm{T}}s_1) + \Delta \\ &= \hat{\mathbf{w}}^{\mathrm{T}}\sigma(\hat{\mathbf{v}}^{\mathrm{T}}s_1) + \dot{\hat{\mathbf{w}}}^{\mathrm{T}}\tilde{\sigma} + \tilde{\mathbf{w}}^{\mathrm{T}}\tilde{\sigma} + \Delta\end{aligned} \tag{34}$$

Using the Taylor series approximation (28) for $\tilde{\sigma}$, according to the approximation error is

$$\begin{aligned}\tilde{u}_{\mathrm{DNNSMC}} &= \hat{\mathbf{w}}^{\mathrm{T}}\sigma(\hat{\mathbf{v}}^{\mathrm{T}}s_1) + \hat{\mathbf{w}}^{\mathrm{T}}[\sigma'(\hat{\mathbf{v}}s_1)\tilde{\mathbf{v}}s_1 + \mathrm{O}^2(\tilde{\mathbf{v}}s_1)] \\ &\quad + \tilde{\mathbf{w}}^{\mathrm{T}}\tilde{\sigma} + \Delta \\ &= \hat{\mathbf{w}}^{\mathrm{T}}\sigma(\hat{\mathbf{v}}^{\mathrm{T}}s_1) + \hat{\mathbf{w}}^{\mathrm{T}}\sigma'(\hat{\mathbf{v}}s_1)\tilde{\mathbf{v}}s_1 + \varepsilon\end{aligned} \tag{35}$$

where $\varepsilon = \hat{\mathbf{w}}^{\mathrm{T}}\mathrm{O}^2(\tilde{\mathbf{v}}s_1) + \hat{\mathbf{w}}^{\mathrm{T}}\tilde{\sigma} + \Delta$ is assumed to be bounded by $|\varepsilon| \leqslant E^*$, in which $|\cdot|$ is the absolute value.

Remark 3. The main problems of the decoupled sliding-mode control are the requirement of uncertainty system parameters to estimate, chattering phenomena to suppress and disturbance bounds to observe in control efforts. In order to deal with these problems, a DNNSMC system including a NN controller and a hitting controller is investigated in this study. The NN control is used to learn the equivalent control u_{DNNSMC} due to the unknown nonlinear system dynamics and the robust control is designed to restrain the controlled system dynamics on the decoupled sliding surface for all time. The hitting controller, a simple adaptive bound estimation algorithm is also utilized for relaxing the requirement of uncertainty and disturbance bounds in the DSMC. The adaptive bound

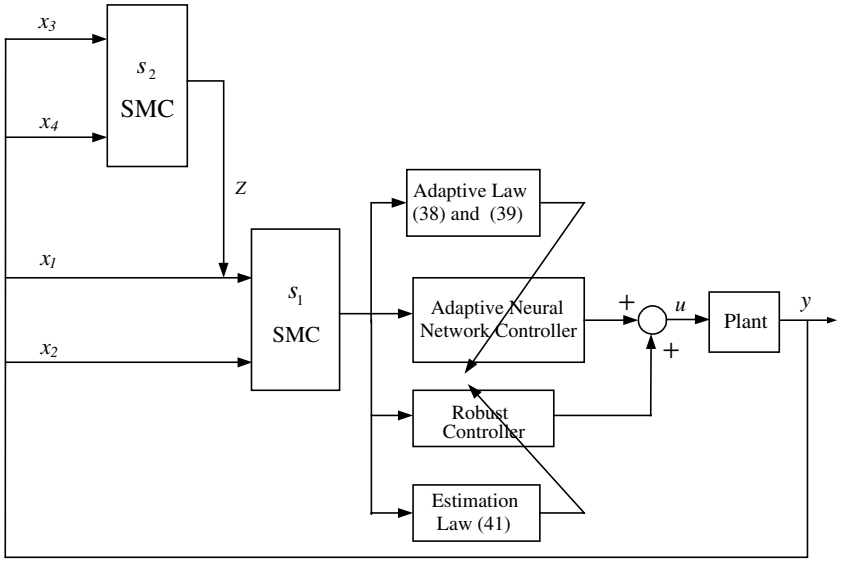

Fig. 2. The DNNSMC system.

estimation designed to adjust the upper bound on the uncertain and disturbance term, can guarantee the tracking error to be zero.

Assumption 1. There exist optimal values for the weight of NN such that

$$\left| u^*_{\mathrm{DNNSMC}} - u_{\mathrm{eq}} + \frac{1}{2} s_\Delta \frac{\partial b_1^{-1}}{\partial \mathbf{x}} \dot{\mathbf{x}} + \varepsilon \right| = E^* \tag{36}$$

where the uncertainty bound E^* is a positive constant.

This uncertainty bound cannot measured for practical applications. Therefore, a bound estimation is developed to observe the bound of approximation error.

$$\Theta = \hat{E}(t) - E^* \tag{37}$$

where $\hat{E}(t)$ is the estimated uncertainty bound. The adaptive laws will be developed to adjust the parameters $\hat{\mathbf{w}}$, $\hat{\mathbf{v}}$ and $\hat{E}$ to estimate $\mathbf{w}^*$, $\mathbf{v}^*$ and E, respectively.

Theorem 1. *Considering the dynamic nonlinear systems described by (2) and the decoupled sliding mode (3), for the bounded, continuous desired state trajectory, if the decoupled neural network sliding mode control law is designed as (29), in which the adaptation laws of the neural network controller are designed as (38), (39) and the robust controller is designed as (40) with the adaptive bound estimation indication in (41), then can guarantee the asymptotic stability of the close-loop system and tracking error will converges to the zero. The decoupled neural network adaptive laws are given by*

$$\dot{\hat{\mathbf{w}}} = \dot{\tilde{\mathbf{w}}} = -\gamma_1 \cdot s_\Delta \cdot \mathrm{sgn}(b_1) \cdot \sigma(\hat{\mathbf{v}} s_\Delta) \tag{38}$$

$$\dot{\hat{\mathbf{v}}} = \dot{\tilde{\mathbf{v}}} = -\gamma_2 \cdot s_\Delta^2 \cdot \mathrm{sgn}(b_1) \cdot \sigma'^{\mathrm{T}}(\hat{\mathbf{v}} s_\Delta) \hat{\mathbf{w}} \tag{39}$$

$$u_h = E \cdot \mathrm{sgn}(b_1) \cdot \mathrm{sat}(s_1/\Phi_1) \tag{40}$$

$$\dot{\hat{E}} = \dot{\Theta} = \gamma_3 \cdot |s_\Delta| \tag{41}$$

where γ_1, γ_2 and γ_4 are positive constants. Moreover, the system states converge to the sliding surface asymptotically.

Proof. Choose the Lyapunov function as

$$V = \frac{1}{2|b_1|} s_\Delta^2 + \frac{1}{2\gamma_1} \tilde{\mathbf{w}}^{\mathrm{T}} \tilde{\mathbf{w}} + \frac{1}{2\gamma_2} \tilde{\mathbf{v}}^{\mathrm{T}} \tilde{\mathbf{v}} \frac{1}{2\gamma_3} \Theta^2 \tag{42}$$

where $\Theta = \hat{E}(t) - E^*$, Φ_1 is the boundary layer thickness, and γ_1, γ_2 and γ_3 are Positive constant. The variation of this function (42) with respect to time is

$$\begin{aligned}
\dot{V} &= \frac{s_\Delta \dot{s}_\Delta}{|b_1|} + \frac{1}{2} s_\Delta^2 \mathrm{sgn}(b_1) \frac{\partial b_1^{-1}}{\partial \mathbf{x}} \dot{\mathbf{x}} + \frac{1}{\gamma_1} \tilde{\mathbf{w}}^{\mathrm{T}} \dot{\tilde{\mathbf{w}}} + \frac{1}{\gamma_2} \tilde{\mathbf{v}}^{\mathrm{T}} \dot{\tilde{\mathbf{v}}} + \frac{1}{\gamma_3} \Theta \dot{\Theta} \\
&= \frac{s_\Delta \dot{s}_\Delta}{|b_1|} + \frac{1}{2} s_\Delta^2 \mathrm{sgn}(b_1) \frac{\partial b_1^{-1}}{\partial \mathbf{x}} \dot{\mathbf{x}} + \frac{1}{\gamma_1} \tilde{\mathbf{w}}^{\mathrm{T}} \dot{\hat{\mathbf{w}}} + \frac{1}{\gamma_2} \tilde{\mathbf{v}}^{\mathrm{T}} \dot{\hat{\mathbf{v}}} + \frac{1}{\gamma_3} \Theta \dot{\hat{E}} \\
&= \frac{1}{|b_1|} s_\Delta (\mathbf{c}^{\mathrm{T}} \dot{\mathbf{x}}_{12} - c_1 \dot{z}) + \frac{1}{2} s_\Delta^2 \mathrm{sgn}(b_1) \frac{\partial b_1^{-1}}{\partial \mathbf{x}} \dot{\mathbf{x}} \\
&\quad + \frac{1}{\gamma_1} \tilde{\mathbf{x}}^{\mathrm{T}} \dot{\hat{\mathbf{w}}} + \frac{1}{\gamma_2} \tilde{\mathbf{v}}^{\mathrm{T}} \dot{\hat{\mathbf{v}}} + \frac{1}{\gamma_3} \Theta \dot{\hat{E}} \\
&= \frac{-k}{|b_1|} s_\Delta^2 + s_\Delta \mathrm{sgn}(b_1) \left(u_{\mathrm{DNNSMC}} + u_h - u_{\mathrm{eq}} + \frac{1}{2} s_\Delta \frac{\partial b_1^{-1}}{\partial \mathbf{x}} \dot{\mathbf{x}} \right. \\
&\quad \left. + \varepsilon + u^*_{\mathrm{DNNSMC}} - u^*_{\mathrm{DNNSMC}} \right) + \frac{1}{\gamma_1} \tilde{\mathbf{w}}^{\mathrm{T}} \dot{\hat{\mathbf{w}}} + \frac{1}{\gamma_2} \tilde{\mathbf{v}}^{\mathrm{T}} \dot{\hat{\mathbf{v}}} + \frac{1}{\gamma_3} \Theta \dot{\hat{E}} \\
&= \frac{-k}{|b_1|} s_\Delta^2 + s_\Delta \mathrm{sgn}(b_1) \left(u^*_{\mathrm{DNNSMC}} - u_{\mathrm{eq}} + \frac{1}{2} s_\Delta \frac{\partial b_1^{-1}}{\partial \mathbf{x}} \dot{\mathbf{x}} + \varepsilon \right) \\
&\quad + s_\Delta \mathrm{sgn}(b_1)(u_{\mathrm{DNNSMC}} - u^*_{\mathrm{DNNSMC}}) + s_\Delta \mathrm{sgn}(b_1) u_h \\
&\quad + \frac{1}{\gamma_1} \tilde{\mathbf{w}}^{\mathrm{T}} \dot{\hat{\mathbf{w}}} + \frac{1}{\gamma_2} \tilde{\mathbf{v}}^{\mathrm{T}} \dot{\hat{\mathbf{v}}} + \frac{1}{\gamma_3} \Theta \dot{\hat{E}} \\
&= \frac{-k}{|b_1|} s_\Delta^2 + s_\Delta \mathrm{sgn}(b_1) \left(u^*_{\mathrm{DNNSMC}} - u_{\mathrm{eq}} + \frac{1}{2} s_\Delta \frac{\partial b_1^{-1}}{\partial \mathbf{x}} \dot{\mathbf{x}} + \varepsilon \right) \\
&\quad + s_\Delta \mathrm{sgn}(b_1)(\tilde{\mathbf{w}}^{\mathrm{T}} \sigma(\hat{\mathbf{v}} s_\Delta) + \hat{\mathbf{w}}^{\mathrm{T}} \sigma'(\hat{\mathbf{v}} s_\Delta) \tilde{\mathbf{v}} s_\Delta - u_h) + \frac{1}{\gamma_1} \tilde{\mathbf{w}}^{\mathrm{T}} \dot{\hat{\mathbf{w}}} \\
&\quad + \frac{1}{\gamma_2} \tilde{\mathbf{v}}^{\mathrm{T}} \dot{\hat{\mathbf{v}}} + \frac{1}{\gamma_3} \Theta \dot{\hat{E}} \leqslant \frac{-k}{|b_1|} s_\Delta^2 + |s_\Delta| E^* + s_\Delta \tilde{\mathbf{w}}^{\mathrm{T}} \sigma(\hat{\mathbf{v}} s_\Delta) \\
&\quad + s_\Delta^2 \hat{\mathbf{w}}^{\mathrm{T}} \sigma'(\hat{\mathbf{v}} s_\Delta) \tilde{\mathbf{v}} - s_\Delta \hat{E} + \frac{1}{\gamma_1} \tilde{\mathbf{w}}^{\mathrm{T}} \dot{\hat{\mathbf{w}}} + \frac{1}{\gamma_2} \tilde{\mathbf{v}}^{\mathrm{T}} \dot{\hat{\mathbf{v}}} + \frac{1}{\gamma_3} \Theta \dot{\hat{E}} \\
&= \frac{-k}{|b_1|} s_\Delta^2 + \tilde{\mathbf{w}}^{\mathrm{T}} \left(\frac{1}{\gamma_1} \dot{\hat{\mathbf{w}}} + s_\Delta \mathrm{sgn}(b_1) \sigma(\hat{\mathbf{v}} s_\Delta) \dot{\hat{\mathbf{w}}} \right) \\
&\quad + \tilde{\mathbf{v}}^{\mathrm{T}} \left(\frac{1}{\gamma_2} \dot{\hat{\mathbf{v}}} + s_\Delta^2 \mathrm{sgn}(b_1) \sigma'^{T}(\hat{\mathbf{v}} s_\Delta) \hat{\mathbf{w}} \right) + \Theta \left(\frac{1}{\gamma_3} \dot{\hat{E}} - |s_\Delta| \right)
\end{aligned} \tag{43}$$

By selecting appropriate values for Φ_1, (38), (39) and (41) implies $\dot{V}$ is negative semidefinite:

$$\dot{V} \leqslant \frac{-k}{|b_1|} s_\Delta^2 \tag{44}$$

If $|s_\Delta| \leqslant \Phi_1$, $s_\Delta = 0$. Then $V = 0$, and $\dot{V} = 0$. If $|s_\Delta| > \Phi_1$ and $\dot{s}_\Delta = \dot{s}_1$ has the same sign as s_1. From the algorithm, we have $s_1 \cdot \dot{s}_1 < 0$. Therefore $\dot{V} = s_1 \cdot \dot{s}_1 < 0$. Then for all $t \geqslant 0$, $\dot{V} \leqslant 0$ holds. So it is a monotonous nonincrease function. Because $\dot{V} \leqslant 0$, $\lim_{t\to\infty} V$ exists, i.e., $V(\infty)$ exists. Then s_Δ is bounded and $\hat{\mathbf{w}}$ and $\hat{\mathbf{v}}$ are bounded too. Since continuous function is bounded in the closed set, so x_i is bounded, and $\dot{s}_\Delta$ is bounded too, and therefore s_Δ is uniform continuous, then $\dot{V} = s_\Delta \cdot \dot{s}_\Delta$ is uniform continuous. Since $V(t)$ is bounded and $\lim_{t\to\infty} \int_0^{\mathrm{T}} \dot{V} \mathrm{d}t = V(\infty) - V(0)$ exists, then by Barbalat lemma (Slotine & Li, 1991), we have $\lim_{t\to\infty} \dot{V} = 0$, and obtain $\lim_{t\to\infty} s_1 = 0$.

In summary, the DNNSMC control law is developed in Eq. (29) with the parameters vector $\hat{\mathbf{w}}$ and $\hat{\mathbf{v}}$ adjusted by (38) and (39). The objective is to construct an adaptive control scheme for unknown dynamic nonlinear plants without using a model of the plant. The proposed approach is NN based with adaptive law combining the decoupled sliding-mode control. Here, no prior knowledge of the plant is assumed, and the controller has to begin with exploration of the state space. The DNNSMC controller ensures Lyapunov stability of the dynamic nonlinear system. □

4. Computer simulation and experimental results

In this section, we shall demonstrate that the DNNSMC is applicable to a single-inverted pendulum system, a doubled-inverted pendulum system, a ball–beam system (Lo & Kuo, 1998) and the practical seesaw system (Liu & Chung, 1997) to verify the theoretical development.

4.1. Single-inverted pendulum

The structure of a single-inverted pendulum is illustrated in Fig. 3 and its dynamic is described below:

$$\begin{aligned}
\dot{x}_1 &= x_2 \\
\dot{x}_2 &= \frac{m_t g \sin x_1 - m_p L \sin x_1 \cos x_1 x_2^2 + \cos x_1 \cdot u}{L \cdot \left(\frac{4}{3} m_t - m_p \cos^2 x_1\right)} + d \\
\dot{x}_3 &= x_4 \\
\dot{x}_4 &= \frac{\frac{4}{3} m_p L x_2^2 \sin x_1 + m_p g \sin x_1 \cos x_1}{\frac{4}{3} m_t - m_p \cos^2 x_1} \\
&\quad + \frac{4}{3 \cdot \left(\frac{4}{3} m_t - m_p \cos^2 x_1\right)} u + d
\end{aligned} \tag{45}$$

where

$x_1 = \theta$ the angle of the pole with respect to the vertical axis;
$x_2 = \dot{\theta}$ the angle velocity of the pole with respect to the vertical axis;
$x_3 = x$ the position of the cart;
$x_4 = \dot{x}$ the velocity of the cart;
$m_t =$ $m_c + m_p$.

In what follows, we define the following variables:

$$s_1 = c_1(\theta - z) + \dot{\theta} = c_1(x_1 - z) + x_2 \tag{46}$$

$$s_2 = c_2 x + \dot{x} = c_2 x_3 + x_4 \tag{47}$$

and

$$z = \text{sat}(s_2/\Phi_z) \cdot Z_u, \quad 0 < Z_u < 1 \tag{48}$$

In the simulation, the following specifications are used:

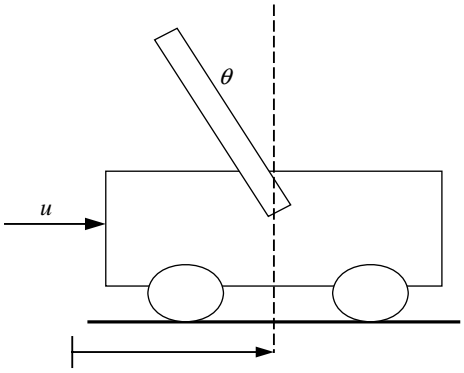

Fig. 3. Structure of a single-inverted pendulum system.

$$m_p = 0.05\ \text{kg}, \quad m_c = 1\ \text{kg}, \quad L = 0.5\ \text{m}$$
$$g = 9.8\ \text{m/s}^2, \quad c_1 = 5, \quad c_2 = 0.5$$
$$\Phi_1 = 5, \quad \Phi_z = 15, \quad Z_u = 0.9425$$
$$|d| \leqslant 0.0873, \quad \gamma_1 = 5, \quad \gamma_2 = 3, \quad \gamma_3 = 1$$

Initial values are

$$\theta = -60^\circ, \quad \dot{\theta} = 0^\circ, \quad x = 0, \quad \dot{x} = 0$$

When the cart moves toward the origin, a larger c_2 makes change s_2 its sign at a position closed to the origin and, accordingly, the force to slow down the cart will be exerted at a position closed to the origin. However, the duration of the action may not be long enough to reduce the speed of the cart to zero, as the cart passes through the origin. The value of c_2 must not be too large, otherwise the cart will be always to swing around the origin. Figs. 4–6 show the simulation results. It is found that the pole and the cart can be stabilized to the equilibrium point. Further, the performance and robustness of proposed control is better than (Chen, Yu, & Chung, 2002; Lo & Kuo, 1998).

4.2. Double-inverted pendulum system

In this section, we shall demonstrate that the proposed control is applicable to the double-inverted pendulum system to verify the theoretical development.

The structure of a double-inverted pendulum system is illustrated in Fig. 7. Pole 1 is the pole connected to the cart and pole 2 is the one above pole 1. The system's dynamics is presented by

$$\begin{aligned}
\dot{x}_1 &= x_2 \\
\dot{x}_2 &= f_1 + b_1 u + d \\
\dot{x}_3 &= x_4 \\
\dot{x}_4 &= f_2 + b_2 u + d \\
\dot{x}_5 &= x_6 \\
\dot{x}_6 &= f_3 + b_3 u
\end{aligned} \tag{49}$$

where

$x_1 = \theta_1$ angle of pole 1 with respect to the vertical axis;
$x_2 = \dot{\theta}_1$ angular velocity of pole 1 with respect to the vertical axis;
$x_3 = \theta_2$ angle of pole 2 with respect to the vertical axis;
$x_4 = \dot{\theta}_2$ angular velocity of pole 2 with respect to the vertical axis;
$x_5 = x$ position of the cart;
$x_6 = \dot{x}$ velocity of the cart

In what follow, we define the following variables:

$$s_1 = c_1(\theta - z) + \dot{\theta} = c_1(x_1 - z) + x_2 \tag{50}$$

$$s_2 = c_2 x + \dot{x} = c_2 x_3 + x_4 \tag{51}$$

$$s_z = c_z x_5 + x_6$$

$$z = \text{sat}(z_l) \cdot Z_u, \quad 0 < Z_u < 1 \tag{52}$$

$$z_l = \begin{cases} -s_z/\Phi_z & \text{if } s_2 \leqslant |s_t| \\ s_2/\Phi_2 & \text{if } s_2 > |s_t| \end{cases} \tag{53}$$

where s_t is the threshold value of s_2.

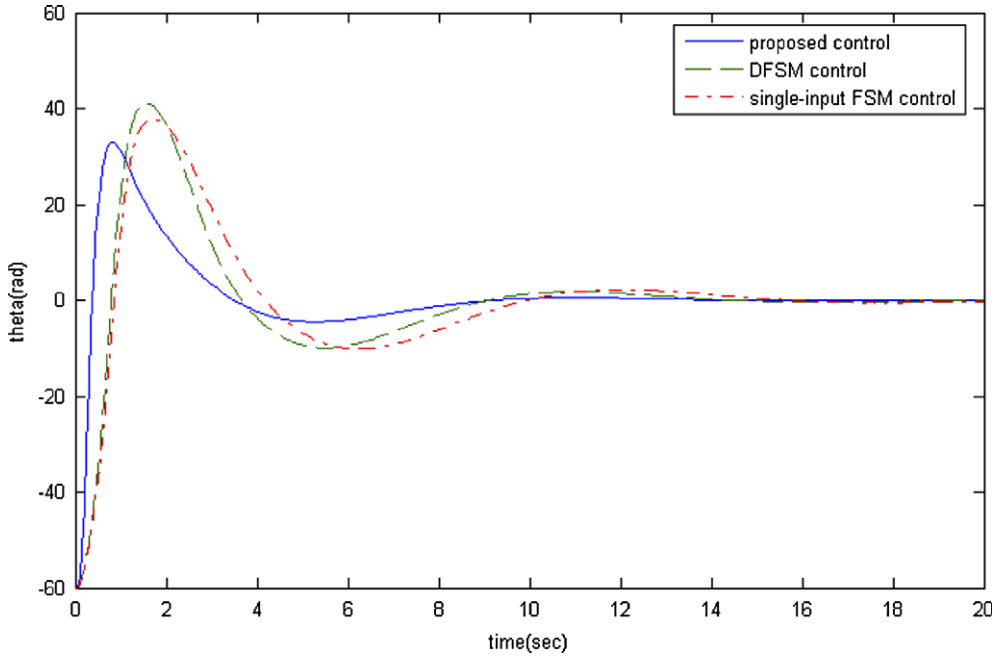

Fig. 4. Angle evolution of the pole.

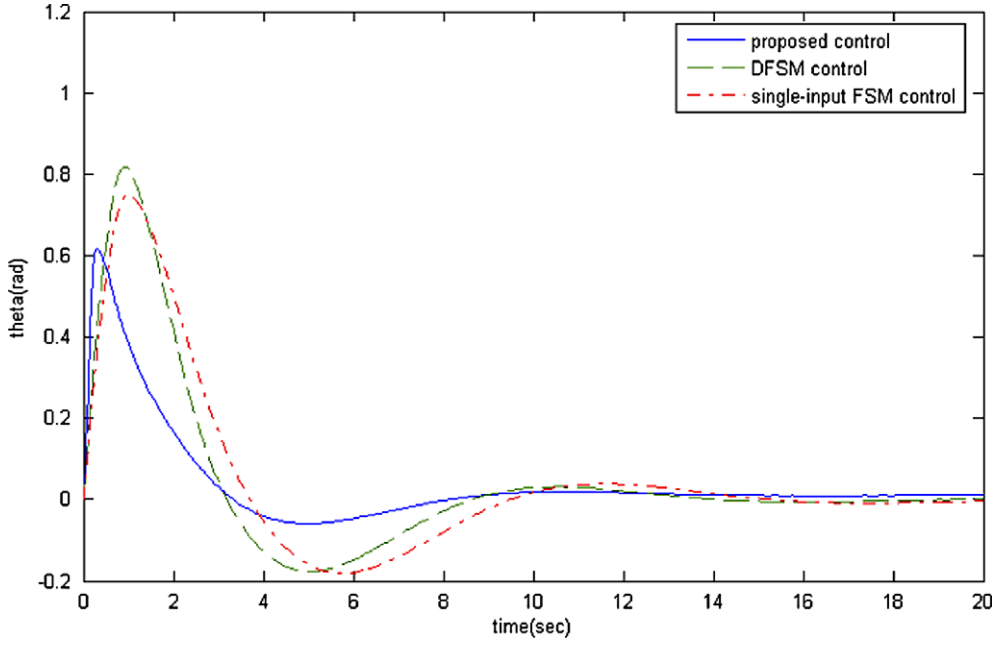

Fig. 5. System intermediate variable z of the single-inverted pendulum system.

In the simulation, the following specifications are used:

$l_1 = 1$ m, $l_1 = 1$ m, $m_1 = 1$ kg, $m_2 = 1$ kg

$m_c = 1$ kg, $L = 0.5$ m, $g = 9.8$ m/s^2, $c_1 = 5$

$c_2 = 1$, $c_z = 0.5$, $\Phi_1 = 5$, $\Phi_2 = 5$, $\Phi_z = 15$

$s_t = 0.01$, $Z_u = 0.4712$, $|d| \leqslant 0.0873$

$\gamma_1 = 5$, $\gamma_2 = 3$, $\gamma_3 = 1$

Initial values are

$\theta_1 = 30^\circ$, $\theta_2 = 10^\circ$, $\ddot{\theta}_1 = \dot{\theta}_1 = 0^\circ$,

$\ddot{\theta}_2 = \dot{\theta}_2 = 0^\circ$, $\ddot{x} = \dot{x} = 0$

The simulation results is found that the pole and the cart can be stabilized to the equilibrium point. Figs. 8–10 show the simulation results. It is found that the pole and cart can be stabilized to the equilibrium point. Further, the

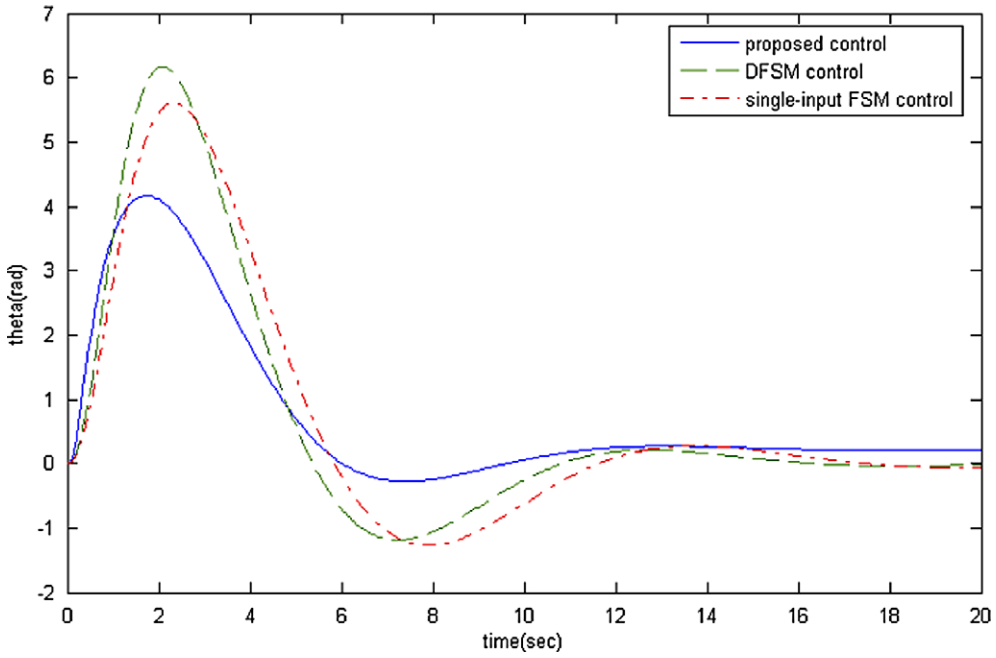

Fig. 6. Position evolution of the cart.

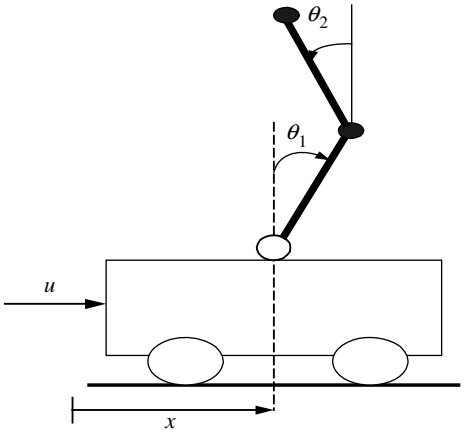

Fig. 7. Structure of a double-inverted pendulum system.

performance and robustness of proposed control is better than (Lin & Mon, 2005; Lo & Kuo, 1998).

4.3. Ball–beam system

Consider a ball–beam system and depicted in Fig. 11 and its dynamic is described below:

$$\begin{aligned}\dot{x}_1 &= x_2\\ \dot{x}_2 &= u + d\\ \dot{x}_3 &= x_4\\ \dot{x}_4 &= B(x_3 x_2^2 - G\sin x_1)\end{aligned} \tag{54}$$

where

$x_1 = \theta$ the angle of the pole with respect to the vertical axis;
$x_2 = \dot{\theta}$ the angle velocity of the pole with respect to the vertical axis;
$x_3 = r$ the position of the cart;
$x_4 = \dot{r}$ the velocity of the cart;
B $\frac{MR^2}{J_b + MR^2}$;
J_b moment of inertia of the ball;
M mass of the ball;
R radius of the ball;
g acceleration of gravity.

The center of rotation is assumed to be frictionless and ball is free to roll along the beam. It is required that the ball remains in contact with the beam and that rolling occurs without slipping. The objective is to keep the ball close to the center of the beam close to the horizontal position.

In the simulation, the following specifications are used:

$$B = 0.7143, \quad J_b = 2 \times 10^{-6}, \quad M = 0.05\ \text{kg}$$
$$R = 0.01\ \text{m}, \quad g = 9.8\ \text{m/s}^2, \quad |d| \leqslant 0.08$$
$$c_1 = 5, \quad c_2 = 0.5, \quad \Phi_1 = 5, \quad \Phi_z = 5$$
$$Z_u = 0.9425, \quad \gamma_1 = 5, \quad \gamma_2 = 3, \quad \gamma_3 = 1$$

Initial values are

$$x_1 = \theta = 60^\circ, \quad x_2 = \dot{\theta} = 0^\circ, \quad x_3 = 10, \quad x_4 = \dot{r} = 0$$

Figs. 12–14 show the simulation results. It is found that the ball–beam can be stabilized to the equilibrium point, and shown that θ and r converge to zero, respectively. Further, the performance and robustness of proposed control is better than (Chen et al., 2002; Lo & Kuo, 1998).

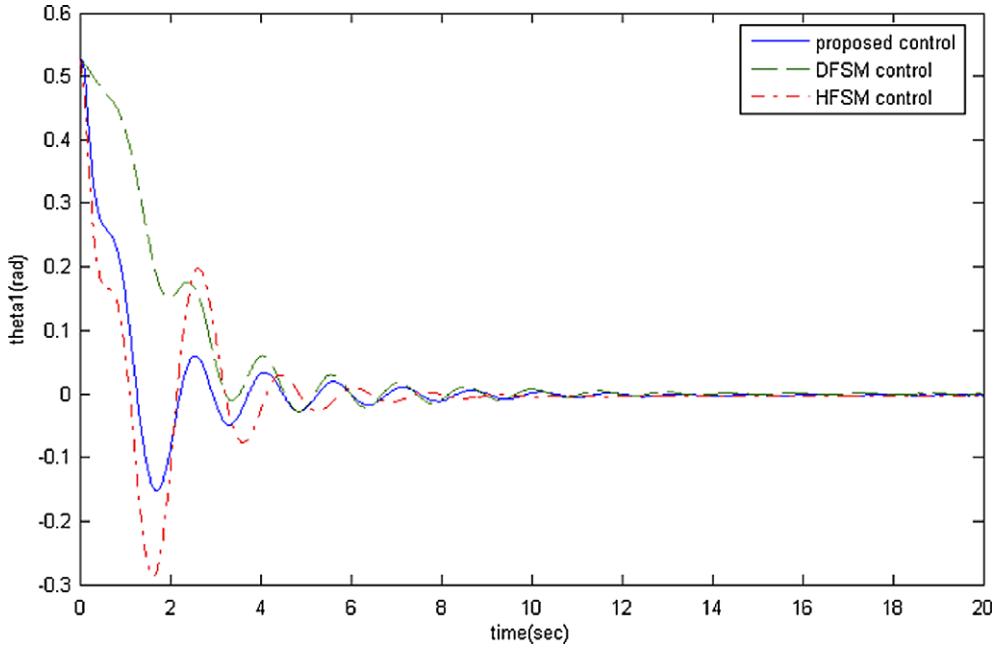

Fig. 8. Angle evolution of the pole 1.

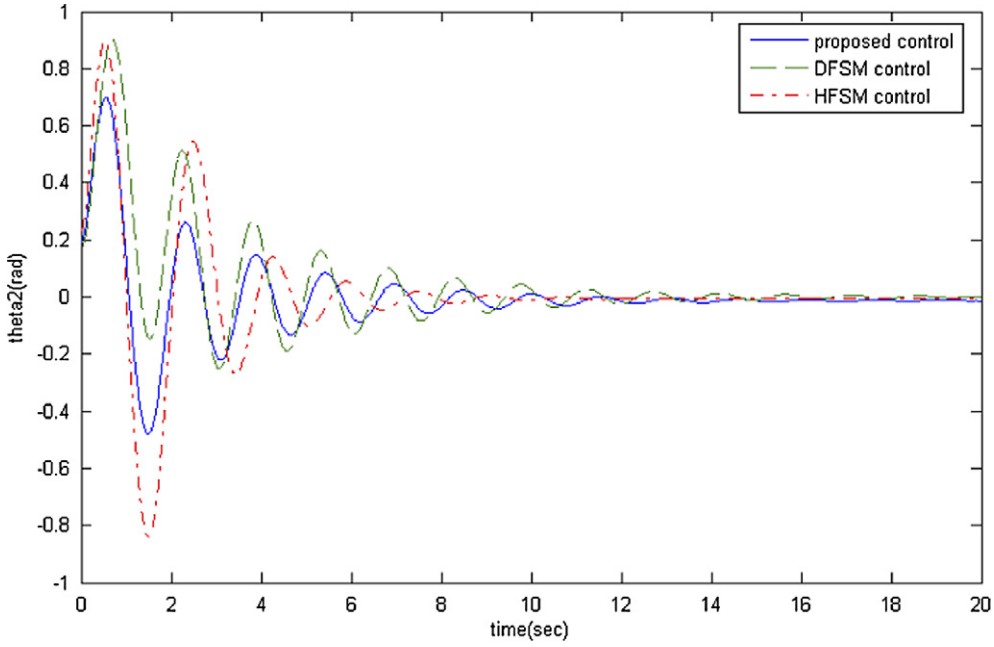

Fig. 9. Angle evolution of the pole 2.

4.4. Seesaw system experimental results

The seesaw consists of a DC Servo Motor, a potentiometer for measuring the seesaw angle, a potentiometer for measuring the cart position, an inverted wedge made of plastic board, a high performance data acquisition card, PCL-818 H, and a 32-bit personal computer (Pentium-133) as a pc-based controller. The balancing mechanism of the seesaw is shown in Fig. 15. The involved parameters of seesaw system are shown in Table 1. In this study, we use the software, Borland C++ Builder (BCB), to design all controllers and to apply the hardware. The previous study gives the system model by using Lagrange's formulations based on principle of balance of force and torque below:

$$\begin{aligned} & m(r_1\ddot{\theta}+\ddot{x})-mx\dot{\theta}^2-mg\sin\theta=uI\ddot{\theta} \\ & \quad +m[r_1(r_1\ddot{\theta}+\ddot{x})+x^2\ddot{\theta}+2x\dot{x}\theta] \\ & \quad -Mgr_2\sin\theta-mg(r_1\sin\theta+x\cos\theta)=0 \end{aligned} \tag{55}$$

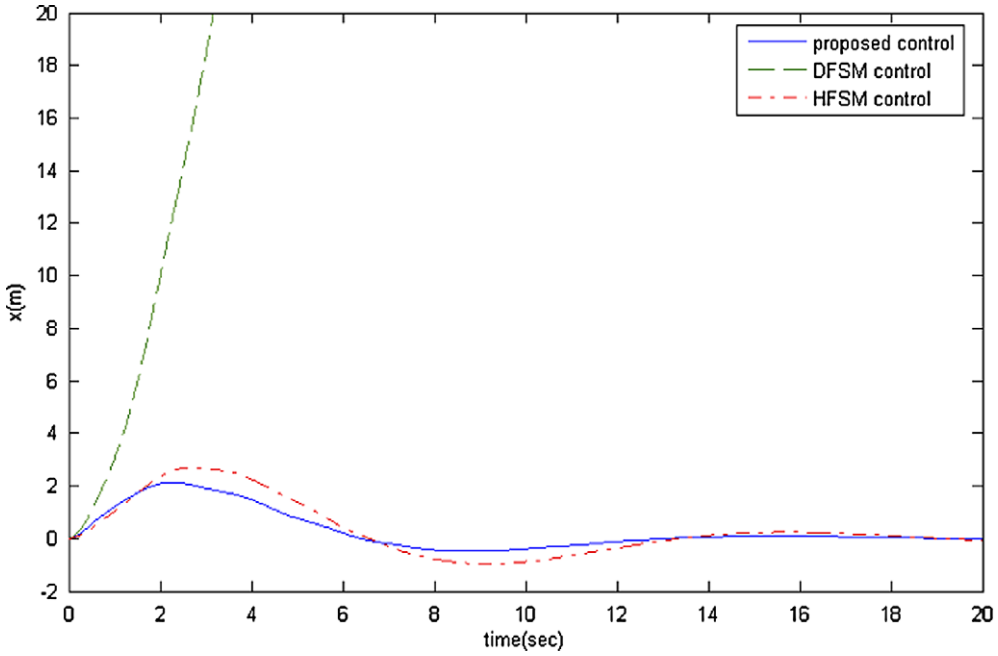

Fig. 10. Position evolution of the cart.

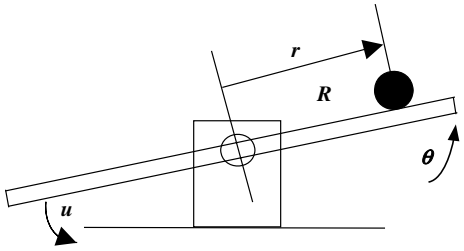

Fig. 11. Structure of a ball beam system.

The dynamical equation of the seesaw mechanism is given as follows:

$$\begin{aligned} &u + mg\sin\theta - B\dot{x} = m\ddot{x} \\ &(Mg\sin\theta)r_2 + mg\sin(\theta + \Phi) \\ &\quad \times \sqrt{(x^2 + r_1^2)} + ur_1 - \mu\dot{\theta} = I\ddot{\theta} \end{aligned} \tag{56}$$

where I is the wedge inertia given by (57)

$$I = M\left(\frac{a^2}{24} + \frac{r_1^2}{2}\right) \tag{57}$$

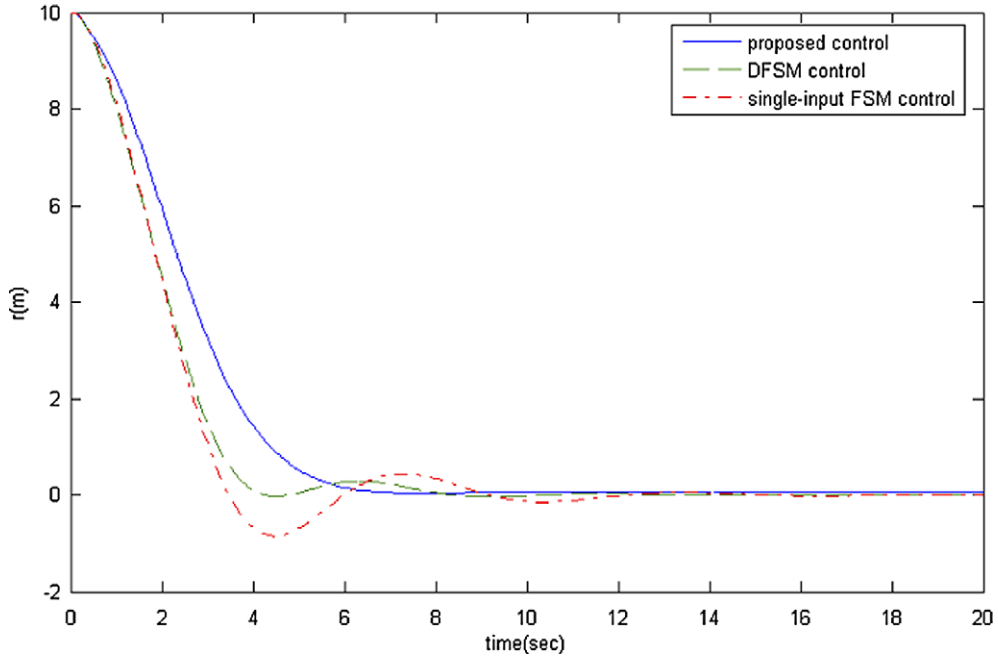

Fig. 12. Position evolution of the ball.

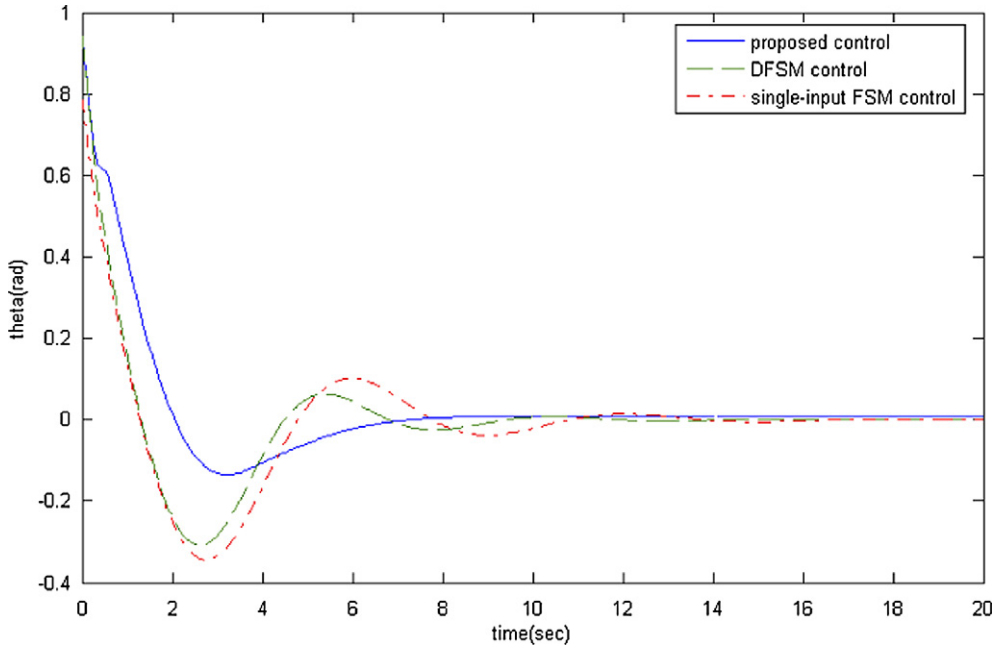

Fig. 13. System intermediate variable z of the ball–beam.

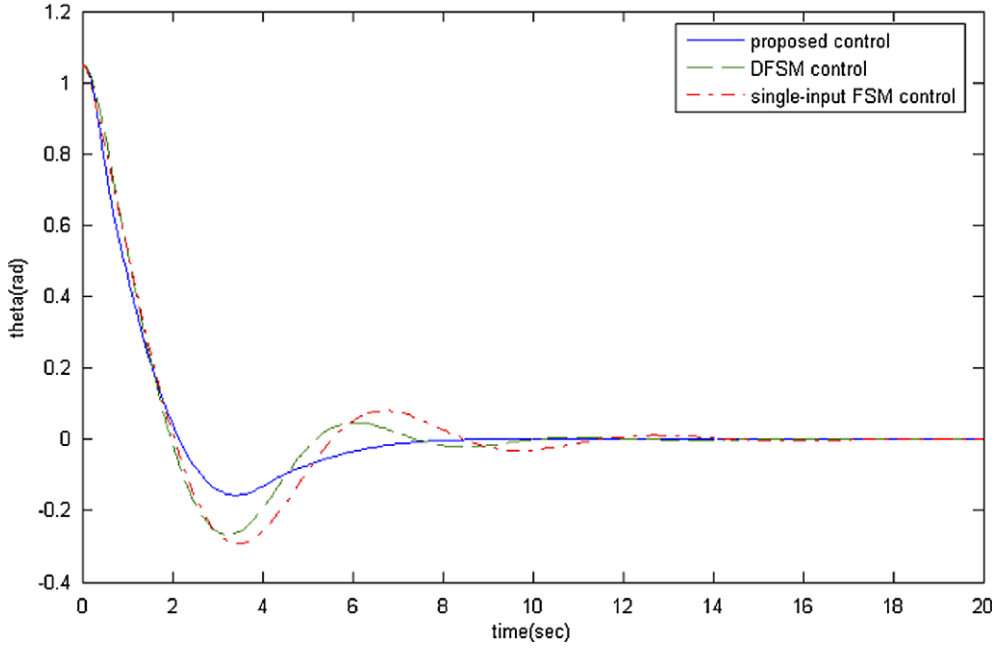

Fig. 14. Angle evolution of the beam.

From Fig. 16, it can be derived below:

$$I = \rho c \int \int (x^2 + y^2)\mathrm{d}x\,\mathrm{d}y$$

$$= \rho c \int_0^b \int_{-\frac{a}{2b}y}^{\frac{a}{2b}y} (x^2 + y^2)\mathrm{d}x\,\mathrm{d}y = \frac{1}{2}\rho abc\left(\frac{a}{24} + \frac{b^2}{2}\right) \quad (58)$$

The parameters of the dynamical equation are denoted. In what follows, we define $x_1 = \theta$, $\dot{x}_2 = \dot{\theta}$, $x_3 = x$, $\dot{x}_4 = \dot{x}$ and

$$s_1 = c_1(\theta - z) + \dot{\theta} = c_1(x_1 - z) + x_2 \quad (59)$$

$$s_2 = c_2 x + \dot{x} = c_3 x_3 + x_4 \quad (60)$$

with

$$z = \mathrm{sat}(s_2/\Phi_z) \cdot Z_u, \quad 0 < Z_u < 1 \quad (61)$$

In the experiment, the following specifications are used:

$$c_1 = 3, \quad c_2 = 0.5, \quad \Phi_1 = 3, \quad \Phi_z = 3, \quad Z_u = 0.4855,$$
$$\gamma_1 = 3, \quad \gamma_2 = 3, \quad \gamma_3 = 2.$$

In this experiment we turn out attention to the performance of the seesaw balance. We want to reduce the settling time and minimize to overshoot and the damping phenomena. The on-line tuning algorithm of parameter is

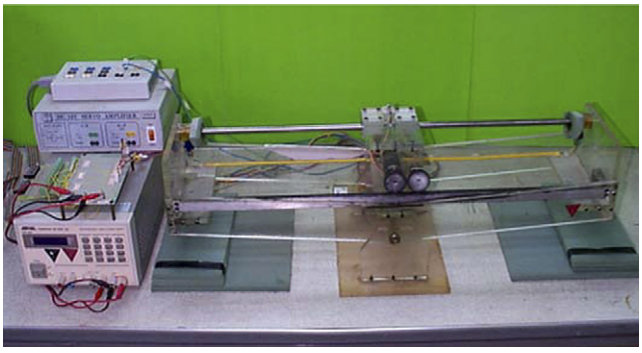

Fig. 15. The practical hardware structure of the seesaw system.

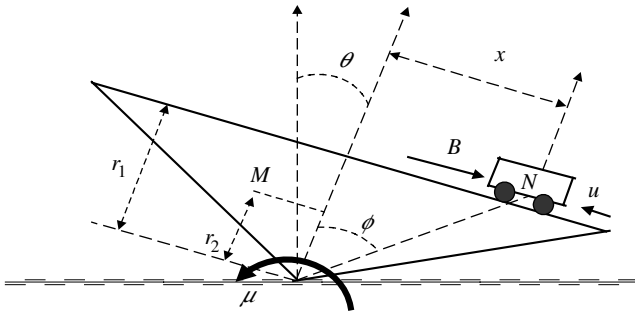

Fig. 16. The balancing mechanism of the inverted wedge.

Table 1
The value of parameters of the seesaw system

Parameter	Value
The inertia of wedge I	0.044
The height of wedge r_1	0.148
The height of center of mass r_2	0.123
The mass of wedge M	1.52
The mass of cart N	0.46
The damping coefficient of the angle	0.3
The damping coefficient of the cart	0.7

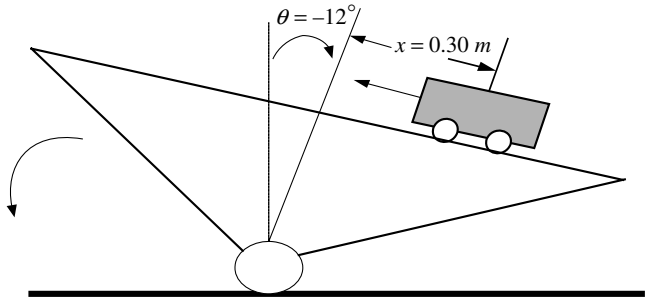

Fig. 17. The initial states of the seesaw of experiment.

proposed to adjust the weight parameters for monitoring the system control performance. The seesaw state variables are cart position (x), cart position change ($\dot{x}$), angle against horizontal (θ), and angle change ($\dot{\theta}$), respectively. The control action based on s_1 is the main one. s_2 is used as an indicator showing how much the cart is away from the origin. If $s_2 > 0$ (locating the cart at the right-hand side of the origin) a negative force is needed to push the cart back to the origin and z must be positive. If $s_2 < 0$, z must be negative.

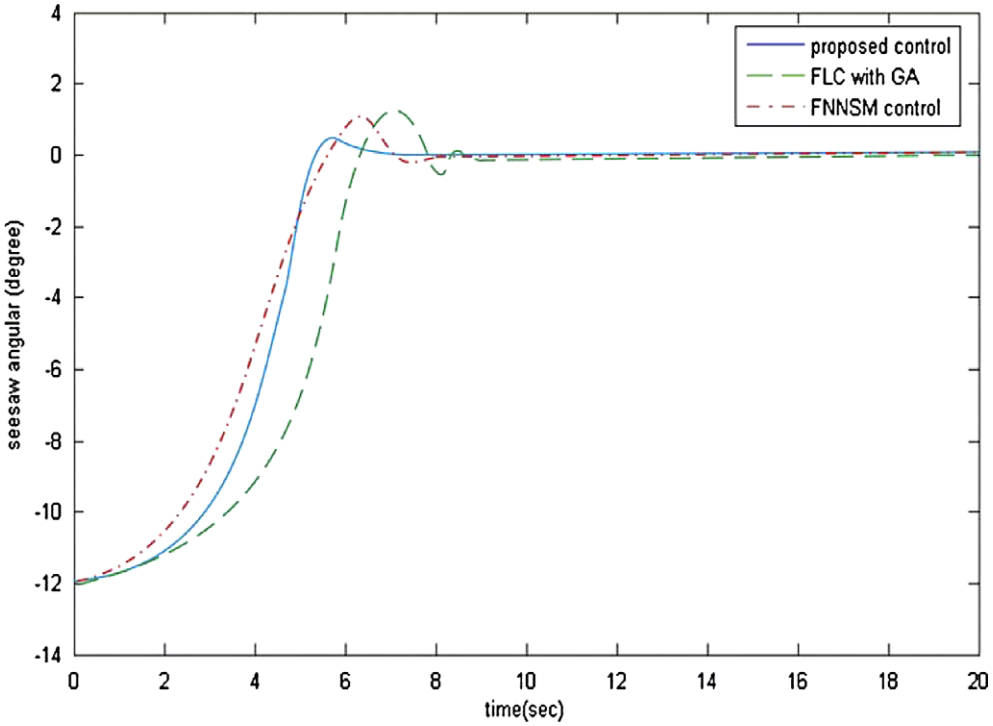

Fig. 18. The angle response of the practical seesaw system.

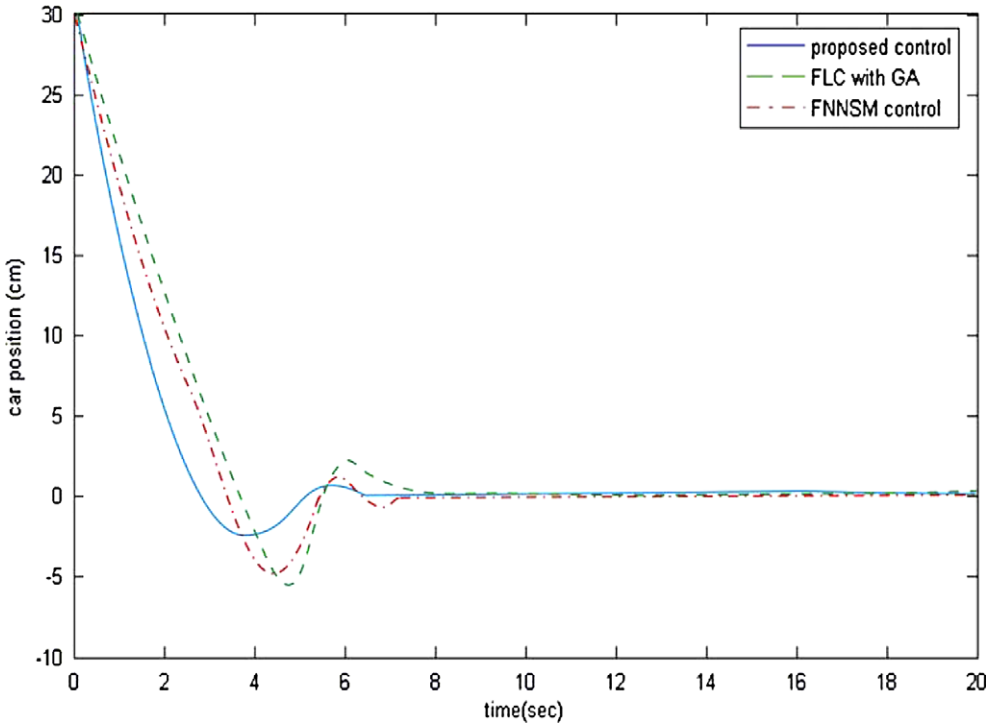

Fig. 19. The position response of the practical seesaw system.

We want to z decrease as decreases, so s_2 can be designed as (13) and to avoid the situation where the cart never stops, c_1 and c_2 must be properly chosen. The initial states of the seesaw is shown on Fig. 17:

The position of the cart x is 30 cm.

The angle of inverted wedge θ is $-12.0°$.

In results of experiment, we detect that the responses position and angle has a similar curve on identical initial states. We compare the DNNSMC, the fuzzy logic controller (FLC) with genetic algorithms (GAs) and the fuzzy-neural network sliding-mode control (FNNSMC) that apply to the identical practical system. Similarly, It is found that the responses position and angle own the same feature under identical initial states. The major advantages of the DNNSMC are that the performance and robust is better than (Liu & Chung, 1997 and Zeng & Chung, 2002), as well as without the exact mathematical model as Figs. 18 and 19. The experiment shows the response performance of FLC with GAs where the initial value of is 30 cm, is $-12°$ and the settling time is 8.4 s. The experiment shows the response performance of FNNSMC where the initial value of is 30 cm, is $-12°$ and the settling time is 7.8 s. The experiment shows the response performance of DNNSMC where the initial value of is 30 cm, is $-12°$ and the settling time is 6.6 s.

5. Conclusions

The decoupled neural network sliding-mode controller has been proposed in this paper. Simulation and experimental results were presented. We use the both decoupled sliding-mode control and NN technique to implement the DNNSMC system. Lyapunov stability theory is used to prove the uniform ultimate boundedness of the states; simulation and experimental results demonstrate the applicability of the proposed method to achieve desired.

The simulation and experimental results have shown that the proposed the NN-based decoupled sliding-mode controller possesses the following advantages:

(1) We do not need to know the mathematical model of the system exactly.
(2) An approximation decoupled sliding-mode control was occurred and the stability of control system can be guaranteed.
(3) The dynamic behavior of the control system can be specified by an user-defined sliding surface.
(4) Does not need any supervise learning procedure. Real time control requirement would be achieved.

.

References

Abdelhameed, M. M., Pinspon, U., & Cetinkunt, S. (2002). Adaptive learning algorithm for cerebellar model articulation controller. *Mechatronics, 12*(6), 859–873.

Barambones, O., & Etxebarria, V. (2002). Robust neural control for robotic manipulators. *Automatica, 38*(2), 235–242.

Barron, A. R. (1993). Universal approximation bounds for superpositions of a sigmoidal function. *IEEE Transactions on Information Theory, 39*(3), 930–945.

Bartolini, G., Punta, E., & Zolezzi, T. (2004). Simplex methods for nonlinear uncertain sliding-mode control. *IEEE Transactions on Automatic Control, 49*(6), 922–933.

Buckner, G. D. (2002). Intelligent bounds on modeling uncertainty: Applications to sliding-mode control. *IEEE Transactions on Systems, Man and Cybernetics, Part C, 32*(2), 113–124.

Chen, T., & Chen, H. (1995). Universal approximation to nonlinear operators by neural network with arbitrary activation functions and its application to dynamical systems. *IEEE Transactions on Neural Network, 6*(4), 911–917.

Chen, S. Y., Yu, F. M., & Chung, H. Y. (2002). Decoupled fuzzy controller design with single-input fuzzy logic. *Fuzzy Sets and Systems, 129*(3), 335–342.

Derks, E. P. P. A., Pastor, M. S. S., & Buydens, L. M. C. (1995). Robustness analysis of radial base function and multi-layered feedforward neural network models. *Chemometrics and Intelligent Laboratory Systems, 28*(1), 49–60.

Horng, J. H. (1999). Neural adaptive tracking control of a DC motor. *Information Sciences, 118*(4), 1–13.

Hornik, K., Stinchombe, M., & White, H. (1989). Multilayer feedforward networks are universal approximators. *Neural Networks, 2*, 359–366.

Huang, S. J., Huang, K. S., & Chiou, K. C. (2003). Development and application of a 27 novel radial basis function sliding-mode controller. *Mechatronics, 13*(4), 313–329.

Huang, S. N., Tan, K. K., & Lee, T. H. (2000). Adaptive friction compensation using neural network approximations. *IEEE Transactions on Systems, Man and Cybernetics, Part C, 30*(4), 551–557.

Hussain, M. A., & Ho, P. Y. (2004). Adaptive sliding-mode control with neural network based hybrid models. *Journal of Process Control, 14*(2), 157–176.

Lin, S. C., & Chen, Y. Y. (1994). RBF-network-based sliding mode control. *IEEE Transactions on Systems, Man and Cybernetics, International Conference on Humans, Information and Technology, 2*, 1957–1961.

Lin, C. M., & Hsu, C. F. (2002). Neural-network-based adaptive control for induction servomotor drive system. *IEEE Transactions on Industrial Electronics, 49*(1), 115–123.

Lin, C. M., & Mon, Y. J. (2005). Decoupling control by hierarchical fuzzy sliding-mode controller. *IEEE Transactions on Control Systems Technology, 13*(4), 593–598.

Liu, Y. R., Chung, H. Y. (1997). Using genetic algorithms design fuzzy logic controllers. M.S. thesis, National Central University, Department of Electrical Engineering.

Liu, P. X., Zuo, M. J., & Meng, M. Q. H. (2003). Using neural network function approximation for optimal design of continuous-state parallel-series systems. *Computers and Operations Research, 30*(3), 339–352.

Lo, J. C., & Kuo, Y. H. (1998). Decoupled fuzzy sliding-mode control. *IEEE Transactions on Fuzzy Systems, 6*(3), 426–435.

Parma, G. G., de Menezes, B. R., & Braga, A. P. (1998). Sliding-mode algorithm for training multilayer artificial neural network. *Electronics Letters, 34*(1), 97–98.

Slotine, J. J. E., & Li, W. (1991). *Applied nonlinear control*. Englewood Cliffs, NJ: Prentice-Hall.

Utkin, V. I. (1977). Variable structure systems with sliding-mode. *IEEE Transactions on Automatic Control, 22*(1), 212–222.

Wai, R. J. (2003). Tracking control based on neural network strategy for robot manipulator. *Neurocomputing, 51*(1), 425–445.

Weibing, G., Wang, Y., & Homaifa, A. (1995). Discrete-time variable structure control systems. *IEEE Transactions on Industrial Electronics, 42*(2), 117–122.

Xu, H., Sun, F., & Sun, Z. (1996). The adaptive sliding-mode control based on a fuzzy neural network for manipulators. *IEEE International Conference on Systems, Man, and Cybernetics, 3*, 1942–1946.

Zeng, J. F., & Chung, H. Y. (2002). Fuzzy sliding mode controllers with applications to seesaw systems. M.S. thesis, National Central University, Department of Electrical Engineering.